Power Electronics and Drives
Volume 11(46), 2026 DOI: 10.2478/pead-2026-0012

Detection of Voltage Asymmetry Based on DC Link Ripple and Analysis of Its Impact on Diagnostic Processes in Complex Electric Drives

Research paper

Stanisław Oliszewski*, Mateusz Dybkowski

Wrocław University of Science and Technology

Received: 12 January, 2026; Received in the revised form: 09 April, 2026; Accepted: 09 April, 2026

Abstract: Voltage imbalance can adversely impact electric motors and other equipment interfaced with a three-phase grid. This phenomenon is prevalent in both industrial power systems and various hybrid vehicle architectures. Faults within the voltage generation system may lead to distortions in the direct current link (DC-link) voltage, thereby compromising the efficacy of fault detection and compensation algorithms in electric drives. Consequently, power supply conditions must be accounted for when developing comprehensive diagnostic frameworks for alternating current (AC) machines. As the voltage asymmetry signatures manifest as specific ripples in the DC-link voltage of systems with an uncontrolled rectifier, detection can be achieved using a single sensor instead of the conventional three-sensor approach. This methodology was proposed and validated through both numerical simulations and experimental testing. Furthermore, the study investigated how variations in DC-link capacitance influence the resulting ripple-based asymmetry factor.

Keywords: *permanent magnet synchronous generator • stator faults • voltage unbalance • power electronics • DC-link*

1. Introduction

AC/DC/AC converters feature a DC-link positioned between the rectifier (AC/DC) and the inverter (DC/AC) stages, which serves as a voltage ripple-damping circuit. Voltage ripples may induce torque pulsations and vibrations in induction motors (Abdul Kadir et al., 2025; Gnaciński et al., 2024), and can further lead to premature electrical insulation failure (Gardan and Montanari, 2024). Consequently, ripple reduction is essential for various applications, including electric vehicle chargers (Jingke et al., 2024), electric motors (Gnaciński et al., 2024), radar systems (Kaboli, 2024) and medical X-ray equipment (Lin et al., 2024). DC-link voltage fluctuations can be exacerbated by capacitor ageing (Jingke et al., 2024) and source voltage unbalance (Oliszewski and Dybkowski, 2024). Such imbalance typically stems from the uneven distribution of single-phase loads (Gnaciński et al., 2024), untransposed transmission lines (Boyd et al., 2024), traction system loads (Pande et al., 2024), and electric vehicle charging (Hasan et al., 2024). Moreover, renewable energy sources may introduce voltage unbalance if proper control of the grid-connected inverters is not applied (Khan et al., 2024). The disturbance in a grid, such as load fluctuations, leads to the voltage imbalance and should be detected, for example, in the frequency domain (Baig et al., 2024) and cross-domain (Baig et al., 2025). Neglecting the analysis of DC voltage quality may result in severe failures of both electric drives and cable insulation.

Voltage unbalance can be identified by applying the fast Fourier transform (FFT) to load current signals (Widagdo et al., 2024). A modified FFT approach (Li et al., 2022) incorporates both phase currents and voltages for detection. Alternatively, unbalance can be detected via the sum and vector of phase voltages (Al-Naimi et al., 2021) or through voltage signals alone using the Generalized Likelihood Ratio Test (Sun et al., 2013). While the methods discussed

* *Email: stanislaw.oliszewski@pwr.edu.pl*

in Al-Naimi et al. (2021); Li et al. (2022); Sun et al. (2013) rely on phase voltage measurements, this paper proposes a detection approach based exclusively on DC-link ripple analysis. This strategy effectively reduces the required number of sensors from three (one per phase) to a single DC voltage sensor. Unlike the already presented single voltage sensor solution (Bogarra et al., 2022), the approach presented in the paper is more focused on the operation mode of the rectifier than the ripple shape.

To sum up the difference between voltage unbalance detection and monitoring methods, a table has been prepared (Table 1). In comparison to the most of the methods, the amount of measurement equipment required is reduced in the provided solution. Moreover, only this method was tested for robustness under the change of DC-link capacitance. On the other hand, method presented in this article requires a relatively high sampling frequency, which is one of the limitations. Another limitation is that the procedure in the manuscript is uncontrolled rectifier-specific.

Table 1. Comparison of voltage unbalance detection and measurement methods.

Article	Signals used	Amount of sensors required	Sampling frequency	Tested for DC-link capacitance change	Uncontrolled rectifier specific
Widagdo et al. (2024)	Load phase currents	3	Unknown	No	No
Li et al. (2022)	Phase voltages	3	8,000 Hz	No	No
Al-Naimi et al. (2021)	Phase voltages	3	1,000 Hz	No	No
Sun et al. (2013)	Phase voltages	3	600 Hz	No	No
Bogarra et al. (2022)	DC-link voltage ripple	1	50,000 Hz	No	Yes
This paper	DC-link voltage ripple	1	10,000 Hz	Yes	Yes

DC-link, direct current link.

1.1. Hybrid vehicle drive system

Hybrid vehicle powertrains are equipped with a three-phase voltage generation system, where the output is rectified by AC/DC converters to charge the battery and supply the DC-link of the frequency converter. The quality of this generated voltage ensures the smooth operation of the electric drive and the reliability of its dedicated diagnostic systems. However, voltage generation units are susceptible to faults, often manifesting as amplitude or phase asymmetries in the sinusoidal output. Stator winding resistance unbalance may arise from manufacturing tolerances or uneven thermal distribution within the windings. Furthermore, short-circuit failures can introduce similar resistance imbalances. Research has shown that such conditions exacerbate harmonic content – if these harmonics are utilised as symptoms for diagnosing stator, bearing, or rotor faults, they may lead to incorrect diagnostic conclusions. Analogous phenomena are observed in stationary industrial drives due to three-phase power grid asymmetries.

Hybrid vehicle powertrains utilise a combination of an internal combustion engine (ICE) and an AC generator across various topologies. Depending on the specific configuration—series, parallel, or power-split (series–parallel)—the energy management strategy varies significantly. This article focuses on the classic series hybrid architecture, the schematic of which is illustrated in Figure 1.

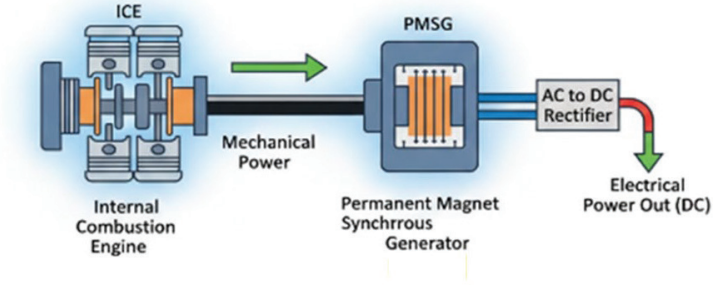

Figure 1. Block diagram of the analysed series hybrid drive architecture. ICE, internal combustion engine; PMSG, permanent magnet synchronous generator.

The system under analysis utilises a permanent magnet synchronous generator (PMSG) coupled with a conventional six-pulse diode rectifier. To isolate phenomena occurring strictly within the DC-link, the study assumes the absence of intermediate DC/DC conversion stages, such as boost or buck converters, at the rectifier output. The comprehensive control architecture, including the rectifier interface, is illustrated in Figure 2.

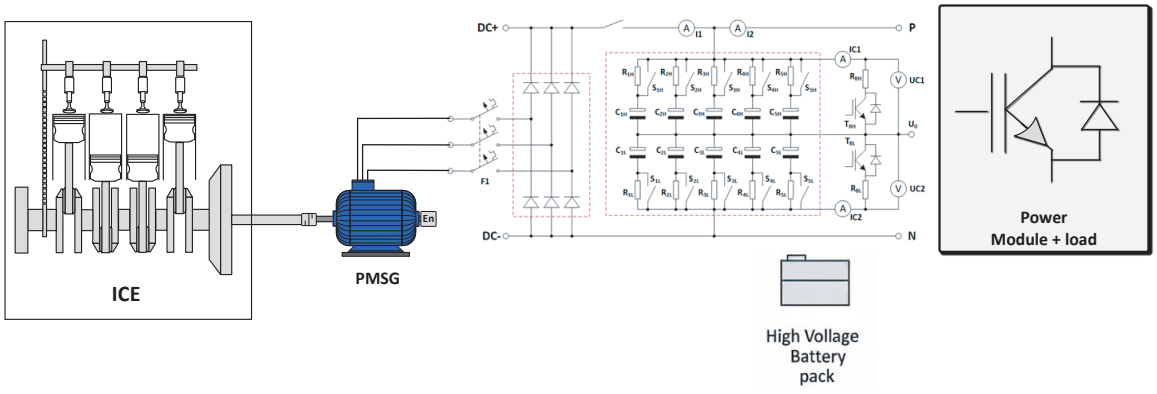

Figure 2. Detailed architecture of the series powertrain featuring a six-pulse rectifier and DC-link circuit. DC-link, direct current link; ICE, internal combustion engine; PMSG, permanent magnet synchronous generator.

The subject of the article is closely related to the issues of Fault Tolerant Control systems (Nesri et al., 2024) and is a supplement to the issues that have been studied for years by the team of authors.

1.2. Aim of the article

This article aims to demonstrate that signal quality issues within the DC-link significantly impact control systems and their associated subsystems. A critical area affected is the fault detection framework for electric motor drives, including induction motors and permanent magnet synchronous motors (PMSMs). Existing literature on drive diagnostics often overlooks external disturbances and secondary faults that can compromise the diagnostic accuracy for operating motors. The motivation behind the research is to utilise as few sensors as possible to obtain reliable voltage unbalance data in the hybrid electric vehicle (HEV) energy generation systems with an uncontrolled rectifier.

As evidenced by recent studies (Pietrzak et al., 2023; Skowron et al., 2022), the vast majority of PMSM fault detection methodologies rely on the frequency analysis of measured signals. Specifically, for demagnetisation (Figure 3), stator (Figure 4) and rotor degradation, the 2nd harmonic of the fundamental supply frequency is frequently considered a primary diagnostic indicator (e.g., 200 Hz in Figure 3 and 100 Hz in Figure 4**).** Furthermore, the 6th harmonic (600 Hz in Figure 4) serves as a significant feature for fault identification.

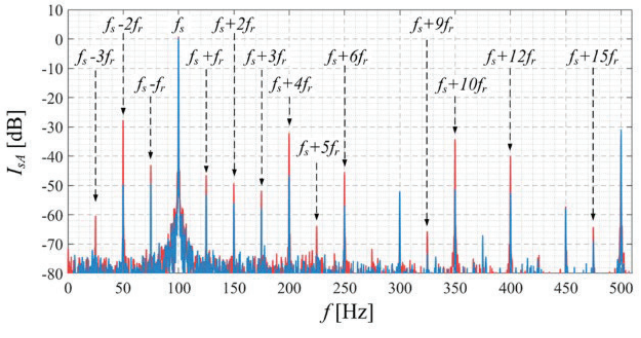

Figure 3. Stator current spectrum - PMSM rotor damage with diagnostic frequencies marked by arrows (Skowron et al., 2022). PMSMs, permanent magnet synchronous motors.

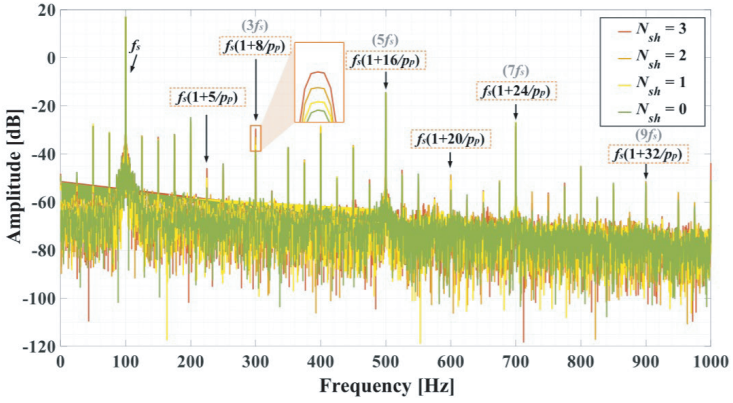

Figure 4. Amplitude of the stator current (spectrum analysis) - PMSM stator damage – *N* meaning the amount of short-circuited winding turns (Pietrzak et al., 2023). PMSMs, permanent magnet synchronous motors.

Diagnostic frameworks for both stator-related and inverter-specific faults rely on harmonic signatures that are inherently dependent on the power source characteristics. Consequently, faults occurring during the PMSG voltage generation stage induce distortions that propagate into the DC-link. The degree to which the AC output deviates from an ideal sinusoid manifests as distinct variations in the harmonic spectrum of the DC-link voltage (U_{DC}). This paper demonstrates that PMSG stator asymmetry—stemming from uneven winding resistances across one or more phases—results in altered higher harmonic content within the DC circuit. These distortions can subsequently lead to the erroneous identification of motor faults, as the control system may misinterpret supply induced ripples as internal motor degradation. Furthermore, this study provides a comparative analysis with three-phase grid asymmetries to demonstrate that these phenomena are analogous to those observed in PMSG-based generation systems.

The purpose and main contribution of this paper is presentation of the DC-link ripple based voltage unbalance detection and assessment solution. The focus is not only the designing method itself but also verifying it under simulation and experimental studies. The potential of this work is the possible implementation of this method in the systems with PMSG and uncontrolled diode rectifiers. Such solution will result in lower costs implementation because of single voltage sensor approach.

2. Initial Simulation Study

To facilitate the preliminary investigation, a MATLAB/Simulink model was developed. The conducted tests focused on variations in DC-link voltage harmonics with respect to various stator resistance asymmetry scenarios. This study allows for the investigation of the phenomenon that is switching from six pulse operation to two pulse one in the uncontrolled AC/DC converters under asymmetrical power supply.

2.1. System model

The simulation model, illustrated in Figure 5, incorporates a PMSG with variable stator phase resistances, a six-pulse diode rectifier, a DC-link, and a resistive–inductive (RL) load. This configuration represents the series HEV architecture (previously shown in Figure 1), where the PMSG and AC/DC converter provide power to the RL load, which emulates the battery pack or subsequent downstream DC/DC conversion stages.

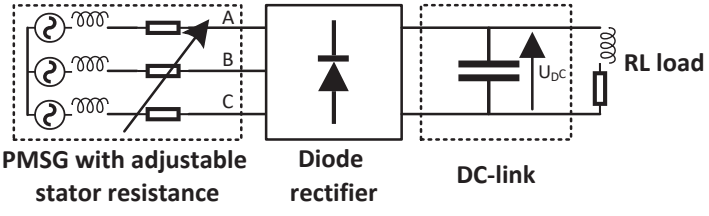

Figure 5. Schematic of the series HEV simulation model. DC-link, direct current link; HEV, hybrid electric vehicle; PMSG, permanent magnet synchronous generator; RL load, resistive–inductive load.

The model was implemented and solved within the MATLAB/Simulink environment. To ensure numerical stability and accuracy, the Backward Euler integration method was employed with a fixed simulation step size of 10^{-7} s.

2.2. Uneven voltage analysis

The initial stage of the simulations involved analysing DC-link voltage variations to characterise the behaviour of the AC/DC system under unbalanced conditions. As illustrated in Figure 6, under balanced supply voltage conditions, the ripples are periodic and regular. The dominant frequency component is observed at 300 Hz, which corresponds to the characteristic ripple frequency of a six-pulse rectifier operating with a 50 Hz AC supply ($6 \times f_{supply}$).

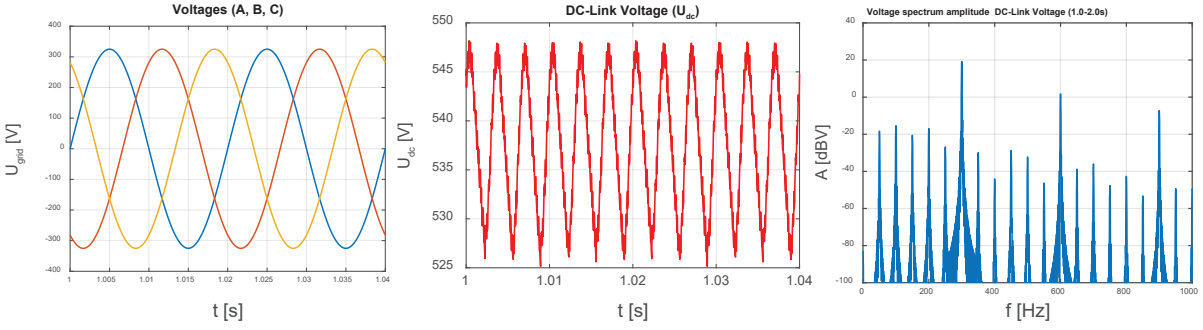

Figure 6. Source and DC-link voltages with frequency spectrum analysis under balanced voltage. DC-link, direct current link.

Increasing the phase *B* voltage by 50% induces a significant voltage source asymmetry, as illustrated in Figure 7. The transition from standard six-pulse operation (characterised by a dominant 300 Hz component) towards a behaviour resembling two-pulse operation (where the 100 Hz component becomes dominant) is clearly discernible in both the U_{DC} time-domain waveforms and the corresponding frequency spectrum. That phenomenon is present in the uncontrolled (diode) rectifiers as the operation of AC/DC converter switches continuous conduction mode to discontinuous one (Fang et al., 2015).

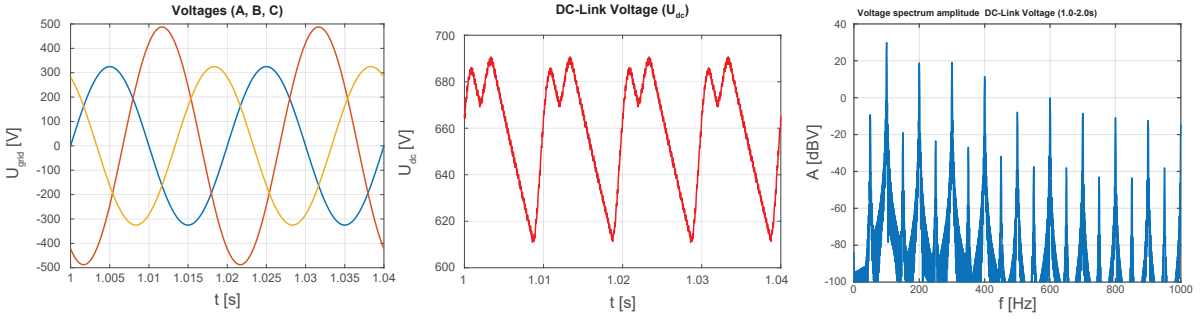

Figure 7. Source and DC-link voltages with frequency spectrum analysis under 50% increase of phase *B* voltage. DC-link, direct current link.

Furthermore, the inclusion of an inverter as the load (Figure 8) does not alter the occurrence of the 100 Hz component - this frequency remains dominant in the presence of voltage asymmetry. This confirms that the characteristic ripple behaviour induced by the source unbalance persists regardless of the load type.

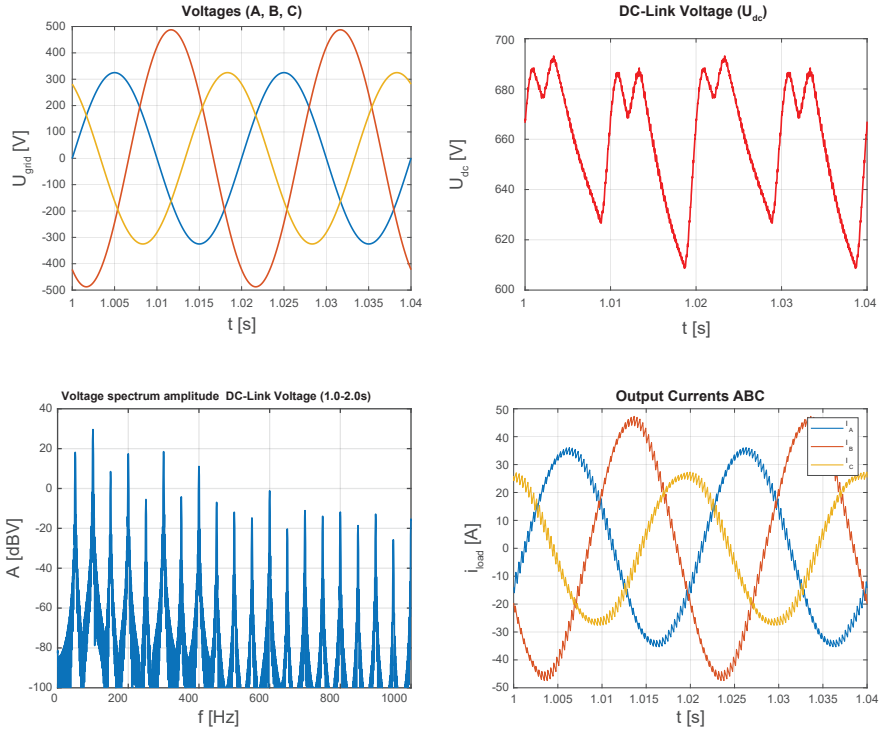

Figure 8. Source, DC-link voltages with frequency spectrum analysis and AC/DC input currents under 50% increase of phase *B* voltage with inverter as a load. AC, alternating current; DC, direct current; DC-link, direct current link.

To enhance the detection of non-linear interactions between harmonic components, a higher-order spectral analysis (HOSA) was conducted. Specifically, the bispectrum of the UDC signal was calculated based on the methodology proposed by Ewert (2020). Unlike the standard power density spectrum (PDS), which only provides information about the power of individual frequency components, the bispectrum preserves phase information and enables the identification of quadratic phase coupling (QPC). In this study, bispectral analysis is utilised to distinguish between inherent rectifier switching harmonics and those induced by supply voltage asymmetries, providing a more robust diagnostic feature than traditional frequency-domain methods. A further bispectral investigation (Figure 9), utilising the methodology proposed by Ewert (2020), demonstrates that increasing voltage asymmetry leads to a more pronounced 100 Hz UDC component relative to the 300 Hz harmonic. This HOSA confirms that the degree of source unbalance is directly correlated with the magnitude of the low-frequency ripple.

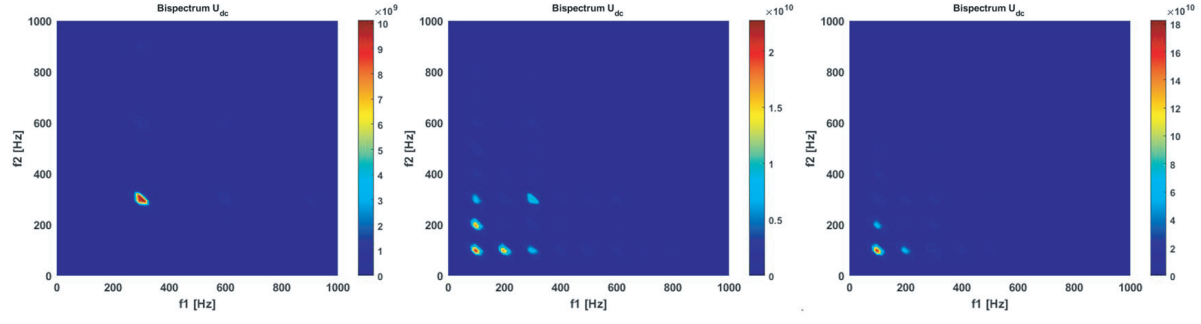

Figure 9. Bispectrum analysis of U_{DC} under changes of phase *B* voltages. From the left: balanced voltage, 120% of phase *B* voltage, 140% of phase *B* voltage.

The bispectrum magnitude is represented on a two-dimensional frequency plane, where the axes f_1 and f_2 denote two independent frequency components. A peak at the coordinates (f_1,f_2) indicate a strong non-linear interaction or QPC between these frequencies and their resultant sum frequency (f_1 + f_2). In the context of the U_{DC} voltage analysis, this allows for a precise observation of how the low-frequency ripples (e.g., 100 Hz) interact with the fundamental switching harmonics (e.g., 300 Hz), providing a more detailed 'fingerprint' of the system's condition than a standard one-dimensional power spectrum. In bispectral analysis of a single signal such as U_{DC}, the frequencies f_1 and f_2 represent coordinates in the bifrequency plane. Although only one physical signal is measured, the bispectrum evaluates the correlation between different spectral components within that signal. Specifically, it identifies QPC, where a peak at (f_1, f_2) indicates that the harmonic component at the sum frequency (f_1 + f_2) is statistically linked to the components at f_1 and f_2. This approach is particularly effective for U_{DC} analysis, as it distinguishes between independent noise and the structured harmonic distortions caused by rectifier non-linearities under supply unbalance.

2.3. Uneven resistance analysis

The 2nd simulation test was conducted based on the considerably high change of PMSG phase *B* resistance R_b. The following analysis is performed in accordance with model schematic on Figure 5 and data presented in Table 2 .

Table 2. Simulation model parameters

Parameters	Value
Stator single phase resistance	2.875 Ω
Stator single phase inductance	9.5 mH
Generator voltage frequency	50 Hz
DC-link capacitance	4.7 mF
Load inductance	1 mH
Load resistance	100 Ω

DC-link, direct current link.

As can be seen in the Figure 10a, the 50% increase in resistance causes the overall U_{DC} mean value to drop. Moreover, the asymmetry between pulses is easily seen – such occurrence increases the lower order harmonics values in the DC-link voltage.

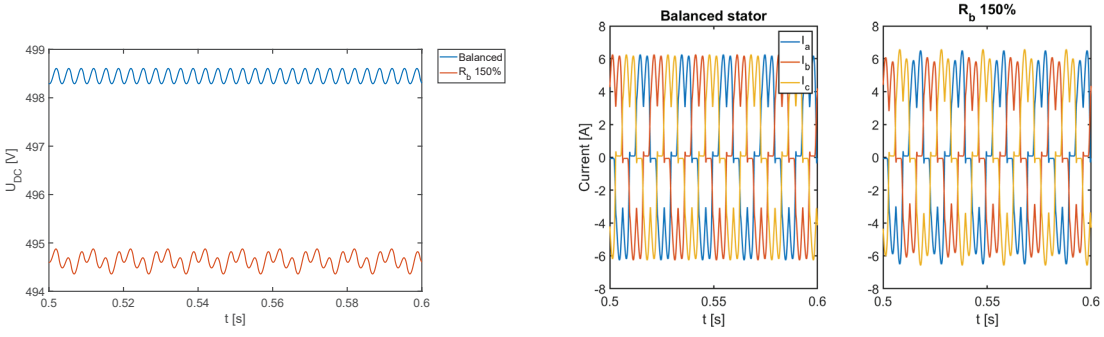

Figure 10. DC-link voltage waveforms for symmetrical stator resistances and increased phase *B* resistance (a) and PMSG stator phase currents under balanced and unbalanced conditions (b). DC-link, direct current link; PMSG, permanent magnet synchronous generator.

In order to understand the resistance asymmetry more deeply, phase currents of PMSG are presented (Figure 10b). The stator resistance unbalance in singular phase causes asymmetrical pulses in each phase current.

The FFT analysis of both cases (Figure 11a) mentioned above provides the information on 50 Hz power supply harmonics structure of U_{DC}. The main 6th harmonic that is reflected by six-pulse operation of the rectifier in the state

of uneven stator resistance is slightly smaller due to the lower mean value. The 2nd, 4th and 8th harmonics increase substantially in comparison to symmetrical stator winding. Those changes will affect diagnostic methods mentioned in Skowron et al. (2022) and Pietrzak et al. (2023).

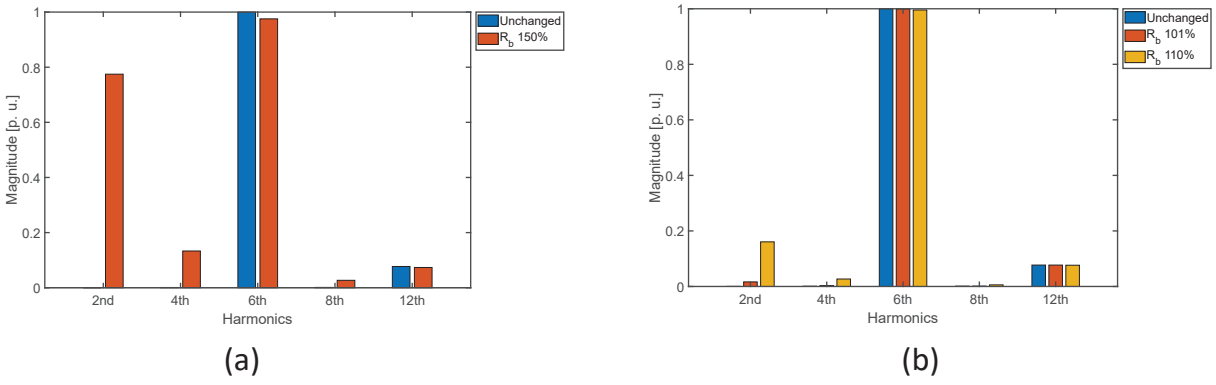

Figure 11. Comparison of U_{DC} harmonic amplitudes under different levels of phase *B* resistance asymmetry: (a) 50% resistance increase, (b) 1% and 10% resistance increase.

Further investigation was undertaken by applying smaller R_b changes (Figure 11b). Even resistance changes as low as 1% can be easily noticed in the 2nd harmonic magnitude change. Additionally, the change of 10% can be noticed in the 4th and 8th harmonic. Those observations prove that even low changes in the PMSG stator resistance symmetry can affect U_{DC} frequency spectrum analysis.

In order to analyse resistance unbalance even further, multiple uneven stator resistances were implemented (Figure 12). In case of the multiple phase asymmetry, as in the single one, harmonics of lower order than six (related to six-pulse rectifier operation) increase, indicating unbalanced source resistances.

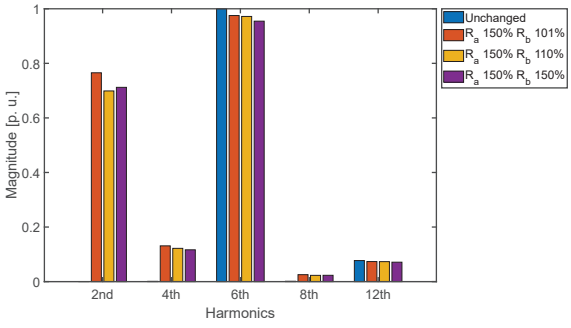

Figure 12. Comparison of harmonics values of U_{DC} while multiple phases resistance change.

3. Experimental Analysis

For the experiment, setup with the possibility to change phase voltages individually (Figure 13) was constructed. Moreover, full AC/CD/AC converter is implemented with induction motor as a load.

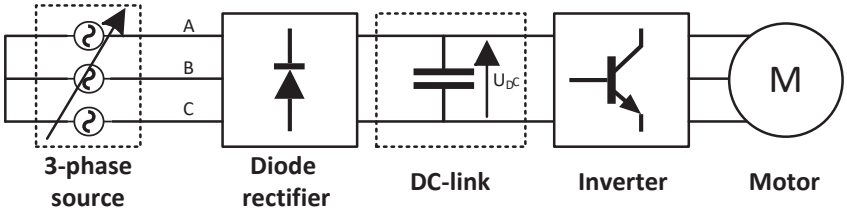

Figure 13. Schematic of experimental setup. DC-link, direct current link.

3.1. Test setup

The experimental bench consists mainly of adjustable voltage source in form of three autotransformers (Figure 14a) and AC/DC/AC converter (Figure 14b). Each autotransformer allows for independent phase voltage adjustment – making it possible to emulate source generator stator resistance asymmetry. AC/DC/AC converter provides load behaviour similar to real industrial scenarios. U_{DC} is measured using differential probe. Signals are recorded using dSpace 1103 with sampling frequency of 10 kHz.

(a) (b)

Figure 14. Test setup core components: three autotransformers (a) and AC/DC/AC converter (b). AC, alternating current; DC, direct current.

3.2. Performed actions

Experiment was conducted under various phase voltage values – each unbalance case was measured at 30 separate sessions in order to obtain satisfactory amount of data for method validation. During each session, harmonic magnitudes are extracted from the DC ripple data using FFT. After obtaining 30 individual frequency spectrum data, mean value for 2nd, 4th, 6th, 8th and 12th harmonics are calculated. Afterwards the procedure continues until all of desired voltage configurations are tested. The flowchart of the experiment can be seen in Figure 15.

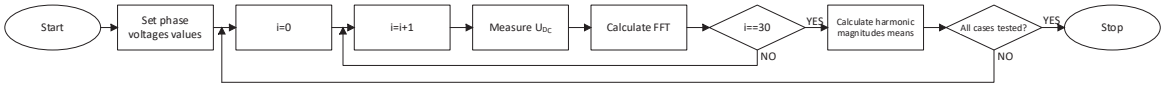

Figure 15. Experiment flowchart.

3.3. Results of experiment

Initially, the balanced state of power supply is considered 100 V root mean square per each phase. In order to represent the physical analogy of stator resistance increase, phase voltage is lowered (e.g., phase *B* in Figure 16). The effect on the U_{DC} is the same as in the Figure 10a – mean DC value is lower and pulses of it are uneven.

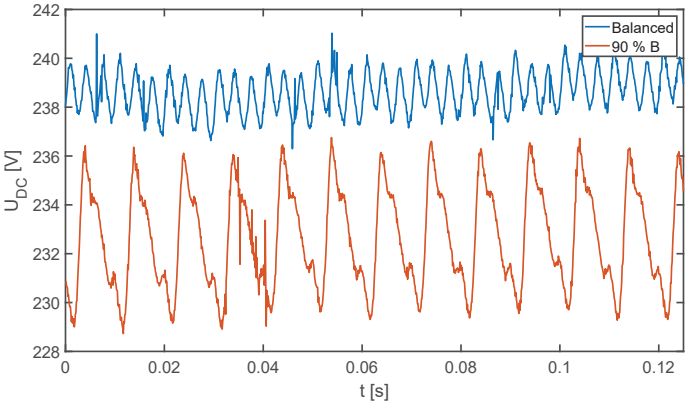

Figure 16. Waveforms of U_{DC} under DC-link *B* phase voltage change. DC-link, direct current link.

During the 1st stage of experimental study, the change of phase *B* voltage is investigated (Figure 17a). The analysis of obtained data FFT proves the results of the simulation study – as the unbalance increases 2nd and 4th harmonics of power supply voltage frequency get higher, worsening the electrical drive operating conditions and affecting other frequency-based diagnostic methods. The presence of mentioned frequency components in the balanced case is because of both power grid and load resistance asymmetries.

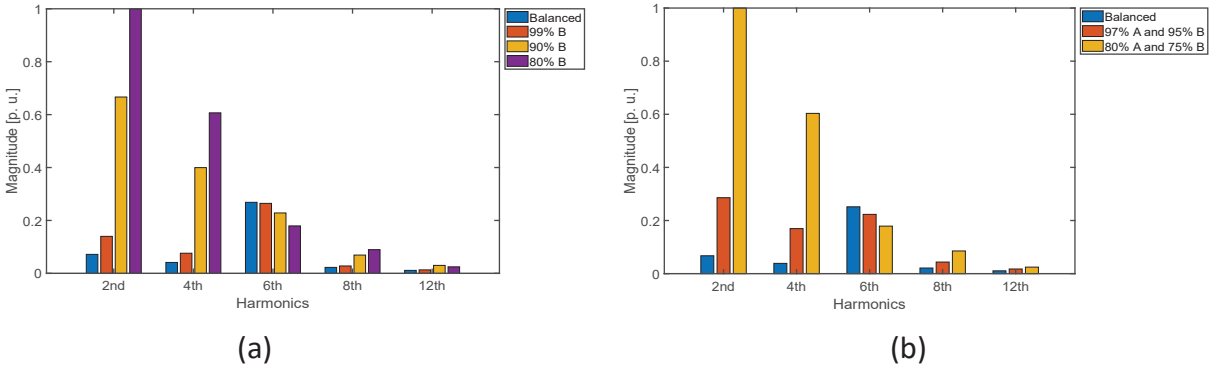

Figure 17. Frequency spectrum of chosen U_{DC} harmonics under different *B* phase voltage values (a) and frequency spectrum of chosen U_{DC} harmonics under different *A* and *B* phase voltage values (b).

In the event of multiple phase voltage unbalance (Figure 17b) the failure mode remains the same – lower than six-pulse related harmonics are amplified.

3.4. FFT and filter approach comparison

Experimental analysis done in Section 3.2 was performed using FFT in order to obtain information on 2nd and 6th harmonics values. The less computationally complex method to perform this task is to use digital bandpass filters that extract desired harmonics (in case presented in paper – 100 Hz and 300 Hz centre frequency). The two applied filters have bandwidth of 20 Hz. By comparing filter-based approach and FFT (Figure 18), it can be seen that for balanced and unbalanced cases, both of harmonics value assessment methods provide similar results.

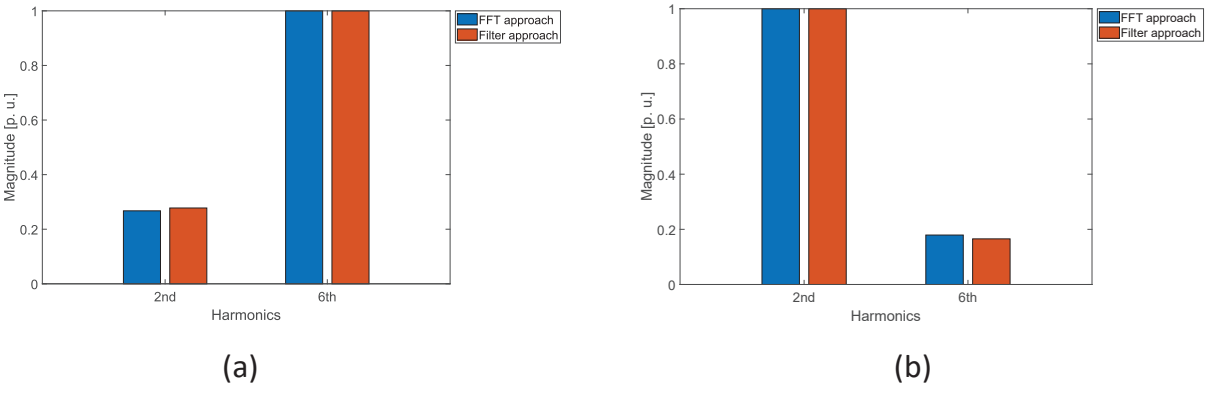

Figure 18. Frequency spectrum of chosen U_{DC} harmonics under balanced (a) and unbalanced (b) condition. FFT, fast Fourier transform.

The complexity comparison was carried out by calculating mean execution time value of 270 runs of the both algorithms for one calculation required to obtain data (one FFT with harmonic indexing and single filtration of 2nd harmonic). In case of filter approach the mean execution time is 68 μs, as opposed to FFT solution where mean time is equal to 439 μs.

Such approach can also be implemented using analogue filters which may be incorporated into smart gate drivers as a power converter diagnostic expansion.

4. Diagnostic Method

Based on the simulation and experimental analysis, the change of 2nd harmonic magnitude in comparison to the progressing source voltage unbalance is a satisfactory diagnostic indicator because of its high and easily noticeable values. It is important to correlate 2nd harmonic with the 6th which is changing less in comparison to the source asymmetry. By doing so, false detection that would occur in the situation of DC-link capacitor change which affects all of the ripples with similar level can be avoided. Using the provided frequency spectrum data voltage ripple unbalance factor (VRUF) was established, which is expressed as:

$$\mathrm{VRUF} = \frac{U_{DC2h}}{U_{DC6h}} \tag{1}$$

where U_{DC2h} is 2nd harmonic magnitude and U_{DC6h} is 6th one.

The theoretical background of the 2nd harmonic to 6th ratio as the unbalance indicator can be found in different uncontrolled rectifier operating modes under the voltage unbalance (Fang et al., 2015). In the balanced state, the rectifier operates in the three-phase continuous conduction mode, meaning that six-pulse operation responsible for the 6th harmonic ripple is present. As the imbalance strengthens, the conduction mode becomes discontinuous and starts to operate with less phases leading ultimately to a single-phase discontinuous conduction mode. That mode manifests itself as the two-pulse rectifier in which the 2nd harmonic is the main ripple contributor. This approach allows for electrical drive load change robustness as the indicator checks for the change of the rectifier operation mode not ripple amplitude.

In order to verify the VRUF in the shape of (1), the change of the factor is paired with the phase *B* voltage change (Figure 19). As can be seen in the figure below, the VRUF increases as the source unbalance gets higher (lower phase *B* voltage), proving its usability as the voltage unbalance detection symptom. The change of VRUF between 90% and 80% of phase voltage is around two times. For comparison, in Bogarra et al. (2022) voltage unbalance indicator increase of around 2.6 times is reported in the similar case.

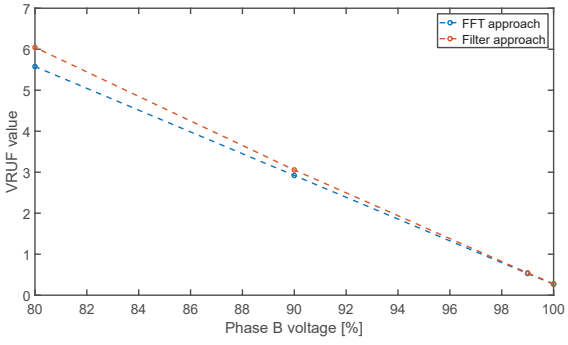

Figure 19. VRUF value in respect to the phase *B* voltage change. FFT, fast Fourier transform; VRUF, voltage ripple unbalance factor.

The experimental setup has a possibility to neglect singular DC-link capacitors by connecting series resistances to them (Figure 2). By doing so, overall DC-bus capacitance can be changed. Different total capacitance values (Table 3) were applied during voltage source balanced state in order to verify the robustness of VRUF under different U_{DC} damping. The choice of the capacitance change is motivated by the fact that as the DC-link capacitors age their capacitance lowers over time affecting the low frequency ripples caused by rectifier operation (Oliszewski et al., 2025). As the U_{DC} voltage ripples change the harmonics used in VRUF also vary, making the DC-link capacitance change robustness test necessary.

Table 3. DC-link capacitance values under the test

Case number	Total capacitance (μF)
1	1175
2	1044
3	940
4	881
5	705

The VRUF value change in respect to the DC-link capacitance in the tested range is around 0.06 units in case of FFT approach (Figure 20). While in respect to the phase *B* voltage change, it is over five units for FFT harmonics extraction (Figure 19). This comparison proves that VRUF does not falsely detect capacitance drop as a AC source asymmetry. As can be seen in Figures 19 and 20, both harmonics filtering and frequency spectrum analysis can be utilised to obtain VRUF.

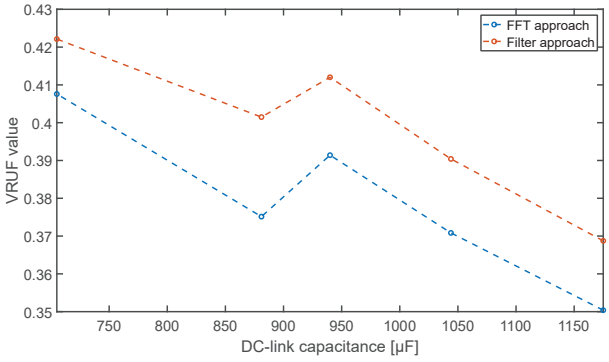

Figure 20. VRUF value in respect to the DC-link capacitance change. DC-link, direct current link;. FFT, fast Fourier transform; VRUF, voltage ripple unbalance factor.

The accuracy of the VRUF was assessed via analysis of its interquartile range (IQR) in relation to the phase *B* voltage change (Figure 21). In the Figure 21 can be seen that VRUF value is consistent and robust to the noise as the value spreads do not overlap each other at different voltage unbalance intensity. Moreover the highest IQR value among both FFT and filter approaches is 0.46 at the 80% of voltage where VRUF value is around 6, proving the solution stability.

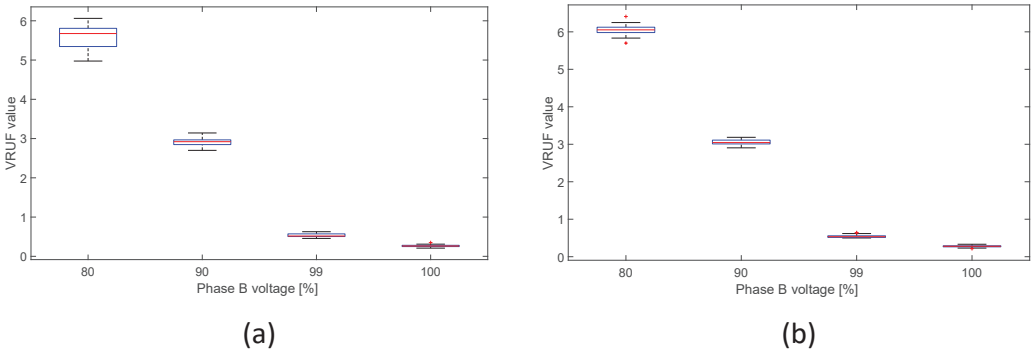

Figure 21. Boxplots of VRUF values for the FFT (a) and filter (b) approaches. FFT, fast Fourier transform; VRUF, voltage ripple unbalance factor.

5. Conclusions

The study presented in this paper focuses on the analysis of U_{DC} voltage ripples in a series HEV powertrain with diode rectifier. The results demonstrate that as the supply voltage unbalance increases, the uncontrolled rectifier operation shifts from a conventional six-pulse characteristic towards a two-pulse behaviour. This transition introduces significant 2nd and 4th harmonics of the fundamental supply frequency into the DC-link, which can compromise the accuracy of electric drive diagnostic systems that rely on frequency spectrum analysis.

The proposed VRUF, based on the ratio between the 2nd and 6th harmonic, provides an effective metric for detecting supply asymmetries. It was shown that the VRUF value increases proportionally with the progression of the asymmetry. This approach enhances the diagnostic reliability of the HEV drive by accounting for the PMSG's influence on DC-link measurements. Furthermore, the VRUF method enables the evaluation of asymmetry levels using only a single voltage sensor on the DC-link, eliminating the need for three separate phase sensors. The robustness of this method has been validated through tests under varying DC-link capacitances, confirming its applicability in real-world operating conditions. In comparison to other unbalance detection methods (Table 1) the requirement of single sensor is the advantage. Moreover, among one sensor solutions it has lower required sampling rate and was tested experimentally for the behavior under different DC-link capacitances. Compared to the other DC-link voltage based unbalance monitoring (Bogarra et al., 2022), the similar magnitude of imbalance indicator change can be observed.

References

Abdul Kadir, M. N., Al-Badrani, H. and Ameen, Y. M. (2025). Model Predictive Control of a New Low Cost 31-Level Inverter. *Power Electronics and Drives*, 10(45), pp. 342–356. doi: 10.2478/pead-2025-0023

Al-Naimi, I. I., Ghaeb, J. A., Baniyounis, M. J. and Al-Khawaldeh, M. (2021). Fast Detection Technique for Voltage Unbalance in Three-phase Power System. *International Journal of Power Electronics and Drive Systems (IJPEDS)*, 12(4), p. 2230. doi: 10.11591/ijpeds.v12.i4.pp2230-2242

Baig, M. A. A., Ratyal, N. I., Amin, A., Jamil, U., Khalid, H. M. and Zia, M. F. (2025). A Multi-Modal Deep Learning Framework for Power Quality Disturbance Classification: An Integration of 1D Time-Series Signals and 2D Scalograms. *Computers and Electrical Engineering*, 128, p. 110716. doi: 10.1016/j.compeleceng.2025.110716

Baig, A., Ratyal, N. I., Amin, A., Jamil, U., Sheroze Liaquat, Khalid, H. M. and Zia, M. F. (2024). An Ensemble Deep CNN Approach for Power Quality Disturbance Classification: A Technological Route Towards Smart Cities Using Image-Based Transfer. *Future Internet*, 16(12), pp. 436–436. doi: 10.3390/fi16120436

Bogarra, S., Saura, J. and Rolán, A. (2022). New Smart Sensor for Voltage Unbalance Measurements in Electrical Power Systems. *Sensors*, 22(21), pp. 8236–8236. doi: 10.3390/s22218236

Boyd, J. D., Reising, D. R., Murphy, A. M., Kuhlers, J. D., McAmis, C. M. and Rossman, J. B. (2024). Machine Learning Techniques to Predict Voltage Unbalance in a Power Transmission System. *IEEE Open Journal of Industry Applications*, 5, pp. 86–93. doi: 10.1109/OJIA.2024.3369993

Ewert, P. (2020). The Application of the Bispectrum Analysis to Detect the Rotor Unbalance of the Induction Motor Supplied by the Mains and Frequency Converter. *Energies*, 13(11), pp. 3009–3009. doi: 10.3390/en13113009

Fang, Z., Cai, T., Duan, S., Chen, C. and Ren, C. (2015). Performance Analysis and Capacitor Design of Three□phase Uncontrolled Rectifier in Slightly Unbalanced Grid. *IET Power Electronics*, 8(8), pp. 1429–1439. doi: 10.1049/iet-pel.2014.0421

Gardan, G. and Montanari, G. C. (2024). AC Ripple on DC Voltage: Experimental and Theoretical Investigation of The Impact on Accelerated Ageing in Electrical Insulation. *High Voltage*, 9(4), pp. 902–910. doi: 10.1049/hve2.12475

Gnaciński, P., Pepliński, M., Muc, A. and Hallmann, D. (2024). Induction Motors Under Voltage Unbalance Combined with Voltage Subharmonics. *Energies*, 17(24), pp. 6324–6324. doi: 10.3390/en17246324

Hasan, M.M., Yousuf, M.A. and Islam, M.R. (2024). Management of EVs for mitigating unbalance in a LV distribution grid. *2024 6th International Conference*

on Electrical Engineering and Information & Communication Technology (ICEEICT), Chengdu, China. pp.1152–1156.

Jingke, C., Junzhong, X., Kaihong, C., Yuxuan, B., Yuxin, Z. and Yong, W. (2024). Output voltage ripple suppression strategy for light DC-link capacitor DC-Type EV charger. In: *2024 IEEE 10th International Power Electronics and Motion Control Conference (IPEMC2024-ECCE Asia)*, Chengdu, China. pp.204–209.

Kaboli, S. (2024). Experimental investigation about the effect of voltage ripple of the power supply on the performance of high power electron tubes. In: *2024 IEEE International Conference on Industrial Technology (ICIT)*, Chengdu, China. pp.1–6.

Khan, M. Z., Haque, A., Malik, A., Amir, M., Zahgeer, F. S. and Khalid, H.M. (2024). A critical review on control techniques for parallel operated inverters in grid connected and standalone mode. *2024 International Conference on Green Energy, Computing and Sustainable Technology (GECOST)*, Chengdu, China. pp.66–71.

Li, D., Gao, Y., Wu, C., Gu, D. and Huang, R. (2022). Voltage Unbalance Factor Detection Based Kaiser- maximum Sidelobe Decay Convolution Window and Amplitude Method. *Electric Power Systems Research*, 204, p. 107705. doi: 10.1016/j.epsr.2021.107705

Lin, C., He, L., Fan, M., Li, X., Fan, S., Wang, C. and Xue, Y. (2024). Output Voltage Ripple Suppression of PPSS-LCC Converter for Medical X-Ray Application Based on Repetitive Control. *IEEE Journal of Emerging and Selected Topics in Industrial Electronics*, 5(4), pp. 1688–1697. doi: 10.1109/JESTIE.2024.3435005

Nesri, M., Benkadi, H., Nounou, K., Sifelislam, G. and Benkhoris, M. F. (2024). Fault Tolerant Control of a Dual Star Induction Machine Drive System using Hybrid Fractional Controller. *Power Electronics and Drives*, 9(1), pp. 161–175. doi: 10.2478/pead-2024-0010

Oliszewski, S. and Dybkowski, M. (2024). Diagnosis of Voltage Unbalance State in a System with Power Converter. *Diagnostyka*, 25(3), pp. 1–7. doi: 10.29354/diag/190567

Oliszewski, S., Pawlak, M. and Dybkowski, M. (2025). DC-Link Capacitors Online Condition Monitoring Using Repetitive RLS in Hybrid-Electric Aircraft. *IEEE Access*, 13, pp. 131166–131176. doi: 10.1109/ACCESS.2025.3591882

Pande, N., Ohnishi, W. and Koseki, T. (2024). Analysis of Voltage Unbalance and Mitigation of Circulating Power in Bilateral Co-phase Traction System. *Electric Power Systems Research*, 228, p. 110048. doi: 10.1016/j.epsr.2023.110048

Pietrzak, P., Wolkiewicz, M. and Orlowska-Kowalska, T. (2023). PMSM Stator Winding Fault Detection and Classification Based on Bispectrum Analysis and Convolutional Neural Network. *IEEE Transactions on Industrial Electronics*, 70(5), pp. 5192–5202. doi: 10.1109/TIE.2022.3189076

Skowron, M., Orlowska-Kowalska, T. and Kowalski, C. T. (2022). Detection of Permanent Magnet Damage of PMSM Drive Based on Direct Analysis of the Stator Phase Currents Using Convolutional Neural Network. *IEEE Transactions on Industrial Electronics*, 69(12), pp. 13665–13675. doi: 10.1109/TIE.2022.3146557

Sun, M., Demirtas, S. and Sahinoglu, Z. (2013). Joint Voltage and Phase Unbalance Detector for Three Phase Power Systems. *IEEE Signal Processing Letters*, 20(1), pp. 11–14. doi: 10.1109/LSP.2012.2226717

Widagdo, R. S., Hermawati, F. A. and Hariadi, B. (2024). Unbalanced Voltage Detection with Measurement Current Signature Analysis (MCSA) in 3-phase Induction Motor Using Fast Fourier Transform (FFT). *Jurnal Teknologi Elektro*, 15(02), pp. 95–101. doi: 10.22441/jte.2024.v15i2.003